Hénon-Heiles System: The Quest to Find a Third Integral of Motion

Fahed Abu Shaer

December 2023

Abstract: In this report, we studied the Hénon-Heiles system of motion, and tried to answer the question whether a third integral of motion exists or no using numerical experiments. We found that the integral existence depends on the initial conditions on the system. Also, we studied the different trajectories that this system produces, the periodic and chaotic ones.

Keywords: Hénon Heiles potential, integral of motion, ergodic behavior, choas, runge-kutta, poincaré map, trajectories, numerical experiments

1 Introduction

In the late 50s and 60s, the question of the existence of a third isolating integral of galactic motion peaked the interest of many Physicists and astronomers around the world. The French astronomer, Michel Hénon, and the American astronomer, Carl Heiles, tried to see whether the integral exist or not in their 1964 paper, *The Applicability of the Third Integral of Motion: Some Numerical Experiments*. They approached the problem using numerical simulations and calculations which we try to attempt in this project.

Hénon and Heiles proposed that the gravitational potential that governs the motion around the galactic center is time-independent and axially symmetric. So, in cylindrical space, the potential is a function of the radius and height of the orbit, $U_g(r, z)$. The phase space, a space that describes all the possible states of the system as a function of the coordinates and their conjugate momenta, has six dimensions, $(r, \dot{r}, \theta, \dot{\theta}, z, \dot{z})$. Therefore, five independent conservative integrals of motions must exist; however, not all of them is isolating. Generally, an integral of motion are relations among the parameters of the problem that is invariant in time, constant in time. They can be isolating or non-isolating. Isolating integrals reduce the dimensions of the trajectory by one, whereas non-isolating integrals don't. In the case of our potential, we have two known isolating integrals of motion, the total energy and the angular momentum.

$$I_1 = U_g(r, z) + \frac{1}{2}m\left(\dot{r} + r^2\dot{\theta}^2 + \dot{z}^2\right) \tag{1}$$

$$I_2 = mR^2\dot{\theta} \tag{2}$$

According to Hénon and Heiles, two of the remaining integrals, I_4 and I_5, can be generally found to be non-isolating. The issue lies in determining whether the third integral is isolating or not. For many years, Physicists, astronomers, and Mathematicians assumed that the third integral is non-isolating because they couldn't express the integral analytically, like I_1 and I_2, despite many attempts. However, observational data suggested otherwise. The observed distribution of stellar velocities near the Sun showed that the dispersion of velocities in the direction towards the galactic center is roughly twice as much as the dispersion in the direction perpendicular to the galactic plane. But, assuming that the third integral is non-isolating predicts that the dispersion is the same in both directions. The model predicted wrong results, so they thought that a third isolating integral must exist then. This invoked a quest to prove the existence or absence of the third isolating integral numerically.

2 Theory

Due to the fact that the angular momentum and energy are integrals of motion, the potential can be expressed in this form,

$$U(r, z) = U_g(r, z) + \frac{J^2}{2mr^2} \tag{3}$$

where J is the constant angular momentum. The equations of motion can expressed as

$$\begin{aligned} m\ddot{r} &= -\frac{\partial U}{\partial r} \\ m\ddot{z} &= -\frac{\partial U}{\partial z} \end{aligned} \tag{4}$$

This is similar to the problem of the planar motion of a particle in an arbitrary potential U. So, we can think of our problem as a particle moving in a plane under the influence of a potential. Hence, we forget momentarily the astronomical origin of the problem and consider the general form to try to answer our question.

Hénon and Heiles suggested to adopt this new formulation and transform the coordinates from r and z to x and y using a transformation that they didn't mention in their paper. So, the phase space now has four dimensions $(x, \dot{x}, y, \dot{y})$ which means there must exist three independent integrals of motion. One of them is the total energy,

$$I_1 = \frac{1}{2}m\left(\dot{x}^2 + \dot{y}^2\right) + U(x, y) \tag{5}$$

The potential has no known symmetries, so the angular momentum is not an integral of motion. It can be also shown that one of the integrals is non-isolating. Therefore, the question arises on the third integral. Since energy is an integral of motion, we can initialize only three coordinates and find the fourth if we have the energy. We start with x, y, and $\dot{y}$ in the phase space, and we find the fourth coordinate $\dot{x}$ using equation (5). The values of $\dot{x}^2$ should be non-negative which give us the condition

$$U(x,y) + \frac{1}{2}\dot{y}^2 \leqslant E \tag{6}$$

This defines a bounded volume. If the trajectory fills the volume, then there is no isolating integral. This is a property of an ergodic behavior where the system over time explores all regions in its phase space, and the trajectory becomes dense and covers the entire available phase space. If the trajectory follows a surface in the volume, then an isolating integral exists.

To visualized the phase space, we consider the successive intersections of the trajectory with the $x = 0$ plane while taking the positive direction upwards. So, the section will show us the trajectory points lying in the $(y, \dot{y})$ plane while satisfying the conditions

$$\begin{aligned} x &= 0 \\ \dot{x} &> 0 \end{aligned} \tag{7}$$

Then, the trajectories in this plane will either follow a curve or fill up the area given by

$$U(0,y) + \frac{1}{2}m\dot{y}^2 \leqslant E \tag{8}$$

The passage from one point to another on the trajectory is called mapping, and this specific map defined by equations (7) is the Poincaré Map.

Hénon and Heiles potential is defined to be

$$U(x,y) = \frac{1}{2}m\omega^2x^2 + \frac{1}{2}m\omega^2y^2 + \frac{m\omega^2}{\Lambda}\left(x^2y - \frac{1}{3}y^3\right) \tag{9}$$

where ω is the harmonic angular frequency and Λ is a constant that has the dimension of length. Hénon and Heiles chose this form of the potential because it is analytically simple which makes the computation of the trajectory easy, yet it is complicated enough to give trajectories which are far from trivial.

In order to make working with this potential easier, we apply a transformation that transforms it to a dimensionless potential while keeping the essential factors. Let the dimension of m, L, and $\frac{1}{\omega}$ to be mass, length, and time, so the dimension of the potential will be $\frac{mL^2}{T^2}$. Consider the following transformations,

$$\begin{aligned} U &= m\omega^2L^2U' \\ x &= Lx' \\ y &= Ly' \end{aligned} \tag{10}$$

where U', x', and y' are the dimensionless potential and coordinates. Apply those transformations on our potential we get,

$$\begin{aligned} U &= \frac{1}{2}m\omega^2x^2 + \frac{1}{2}m\omega^2y^2 + \frac{m\omega^2}{\Lambda}\left(x^2y - \frac{1}{3}y^3\right) \\ m\omega^2L^2U' &= \frac{1}{2}m\omega^2L^2x'^2 + \frac{1}{2}m\omega^2L^2y'^2 + \\ &\quad \frac{m\omega^2}{\Lambda}\left(L^3x'^2y' - \frac{1}{3}L^3y'^3\right) \\ m\omega^2L^2U' &= \frac{1}{2}m\omega^2L^2x'^2 + \frac{1}{2}m\omega^2L^2y'^2 + \\ &\quad \frac{m\omega^2L^3}{\Lambda}\left(x'^2y' - \frac{1}{3}y'^3\right) \\ U' &= \frac{1}{2}x'^2 + \frac{1}{2}y'^2 + \frac{L}{\Lambda}\left(x'^2y' - \frac{1}{3}y'^3\right) \end{aligned}$$

$$U = \frac{1}{2}x^2 + \frac{1}{2}y^2 + \eta\left(x^2y - \frac{y^3}{3}\right) \tag{11}$$

where η is a dimensionless constant that is a measure of non-linearity. Hénon and Heiles chose $\eta = 1$, and we will too.

The figures below show the Hénon and Heiles (HH) potential in different views. Figure 1 shows the potential plotted in three dimensions $(x, y, U(x,y))$. While figure 2 shows us the potential in the (x, U) plane, when $y = 0$. The potential look like a parabola just like that of a harmonic oscillator. Lastly, figure 3 shows the potential in the (y, U) plane, when $x = 0$. So, it can be said that the HH potential is two isotropic harmonic oscillators coupled by the perturbation terms.

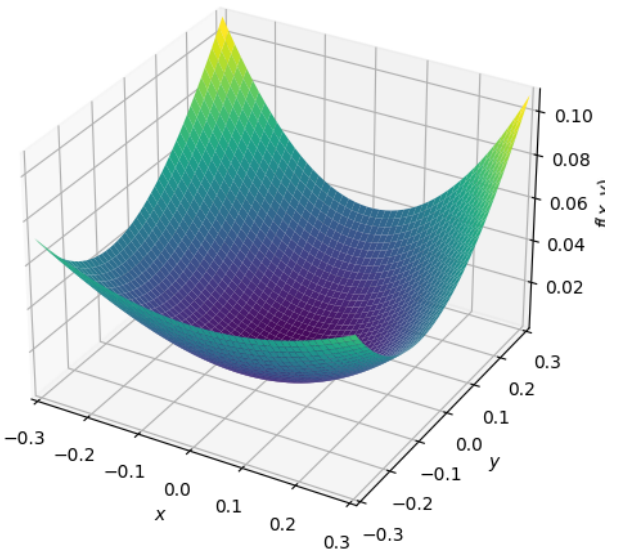

Figure 1: Hénon Heiles Potential in 3D

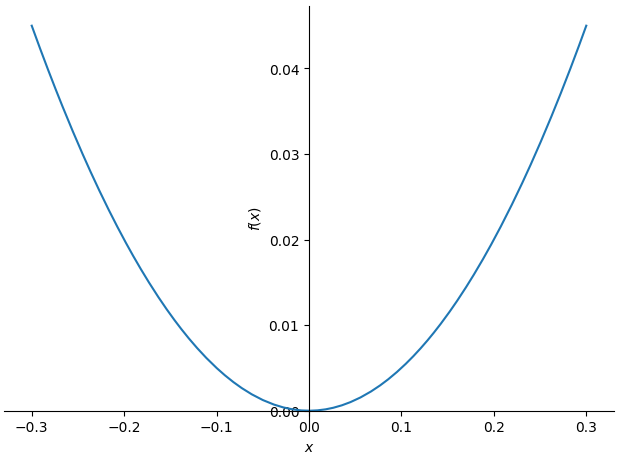

Figure 2: Hénon Heiles Potential when $y = 0$

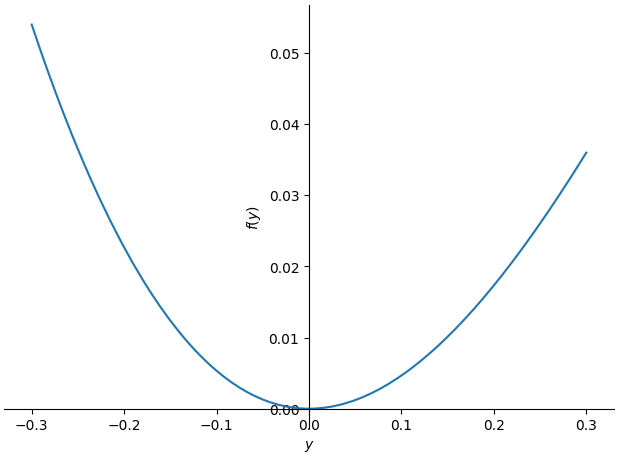

Figure 3: Hénon Heiles Potential when $x = 0$

We find the fixed points of the potential analytically. First, we take the first derivatives with respect to x and y.

$$\begin{cases} \partial V_x = x + 2xy \\ \partial V_y = y + x^2 - y^2 \end{cases} \tag{12}$$

To find the fixed points, we equate the derivatives to zero, so

$$\begin{cases} x + 2xy = 0 \\ y + x^2 - y^2 = 0 \end{cases} \tag{13}$$

Working on the first equation of the system,

$$\begin{aligned} x + 2xy &= 0 \\ x(1 + 2y) &= 0 \end{aligned}$$

$$x = 0 \text{ or } y = -\frac{1}{2} \tag{14}$$

If $x = 0$,

$$\begin{aligned} y + x^2 - y^2 &= 0 \\ y - y^2 &= 0 \\ y(y - 1) &= 0 \end{aligned}$$

$$y = 0 \text{ or } y = 1 \tag{15}$$

If $x \neq 0$ and $y = -\frac{1}{2}$,

$$\begin{aligned} y + x^2 - y^2 &= 0 \\ -\frac{1}{2} + x^2 - \frac{1}{4} &= 0 \\ x^2 &= \frac{3}{4} \end{aligned}$$

$$x = \pm\frac{\sqrt{3}}{2} \tag{16}$$

Hence, the fixed points of the Hénon Heiles potential are $\left[(0,0), (0,1), \left(\frac{\sqrt{3}}{2}, -\frac{1}{2}\right), \left(-\frac{\sqrt{3}}{2}, -\frac{1}{2}\right)\right]$.

After finding the fixed points, we now evaluate their stability by evaluating the Jacobian at those points and finding its eigenvalues. If the eigenvalues were positive, then the point is unstable. If the eigenvalues were negative, then the point is stable. If the eigenvalues were a mix of positive and negative values, then the point is a saddle point. Lastly, if the eigenvalues are imaginary, then it is a center.

Let the partial derivative with respect to x, ∂V_x, be $f_1(x, y)$, and the partial derivative with respect to y, ∂V_y, be $f_2(x, y)$, then the Jacobian is,

$$J(x, y) = \begin{pmatrix} \frac{\partial f_1}{\partial x} & \frac{\partial f_1}{\partial y} \\ \frac{\partial f_2}{\partial x} & \frac{\partial f_2}{\partial y} \end{pmatrix}$$

$$J(x, y) = \begin{pmatrix} 1 + 2y & 2x \\ 2x & 1 - 2y \end{pmatrix} \tag{17}$$

Evaluating the Jacobian at $(0, 1)$,

$$J(0, 1) = \begin{pmatrix} 1 + 2 & 0 \\ 0 & 1 - 2 \end{pmatrix} = \begin{pmatrix} 3 & 0 \\ 0 & -1 \end{pmatrix} \tag{18}$$

We find the eigenvalues of this Jacobian,

$$|J - \lambda I| = \begin{vmatrix} 3 - \lambda & 0 \\ 0 & -1 - \lambda \end{vmatrix} = (3 - \lambda)(-1 - \lambda) = 0 \tag{19}$$

Therefore, the eigenvalues of the Jacobian at $(0, 1)$ are $\lambda_1 = 3$ and $\lambda_2 = -1$. The one of the eigenvalues is positive and the other is negative, so this fixed point is a saddle point.

Then, we evaluate the Jacobian at $(\pm\frac{\sqrt{3}}{2}, -\frac{1}{2})$,

$$\begin{aligned} J\left(\pm\frac{\sqrt{3}}{2}, -\frac{1}{2}\right) &= \begin{pmatrix} 1 - 1 & \pm\sqrt{3} \\ \pm\sqrt{3} & 1 + 1 \end{pmatrix} \\ &= \begin{pmatrix} 0 & \pm\sqrt{3} \\ \pm\sqrt{3} & 2 \end{pmatrix} \end{aligned} \tag{20}$$

We find the eigenvalues of this Jacobian,

$$\begin{aligned} |J - \lambda I| = \begin{vmatrix} -\lambda & \pm\sqrt{3} \\ \pm\sqrt{3} & 2 - \lambda \end{vmatrix} &= (-\lambda)(-2 - \lambda) - 3 = \lambda^2 - 2\lambda - 3 \\ &= (\lambda - 3)(\lambda + 1) = 0 \end{aligned} \tag{21}$$

Therefore, the eigenvalues of the Jacobian at $\left(\pm\frac{\sqrt{3}}{2}, -\frac{1}{2}\right)$ are $\lambda_1 = 3$ and $\lambda_2 = -1$. The one of

the eigenvalues is positive and the other is negative, so these fixed points are also saddle points.

Lastly, we evaluate it at the origin $(0,0)$,

$$J(0,0) = \begin{pmatrix} 1 & 0 \\ 0 & 1 \end{pmatrix} \tag{22}$$

We find the eigenvalues of this Jacobian,

$$|J - \lambda I| = \begin{vmatrix} 1-\lambda & 0 \\ 0 & 1-\lambda \end{vmatrix} = (1-\lambda)(1-\lambda) = 0 \tag{23}$$

Therefore, the eigenvalues of the Jacobian at $(0,0)$ are $\lambda_1 = \lambda_2 = 1$. Both eigenvalues are positive, so the fixed point is unstable.

After finding the fixed points, we are going to evaluate the potential at them. First, consider $(0,1)$,

$$V(0,1) = \frac{1}{2}(0)^2 + \frac{1}{2}(1)^2 + (0)^2(1) - \frac{1}{3}(1)^3 = \frac{1}{2} - \frac{1}{3} = \frac{1}{6} \tag{24}$$

Then, we consider $\left(\pm\frac{\sqrt{3}}{2}, -\frac{1}{2}\right)$,

$$\begin{aligned} V\left(\pm\frac{\sqrt{3}}{2}, -\frac{1}{2}\right) &= \frac{1}{2}\left(\pm\frac{\sqrt{3}}{2}\right)^2 + \frac{1}{2}\left(-\frac{1}{2}\right)^2 \\ &\quad + \left(\pm\frac{\sqrt{3}}{2}\right)^2\left(-\frac{1}{2}\right) - \frac{1}{3}\left(-\frac{1}{2}\right)^3 \\ &= \frac{3}{8} + \frac{1}{8} - \frac{3}{8} + \frac{1}{24} = \frac{1}{6} \end{aligned} \tag{25}$$

Since the points $(0,1), \left(\frac{\sqrt{3}}{2}, \frac{1}{2}\right), \left(\frac{-\sqrt{3}}{2}, \frac{1}{2}\right)$ are saddle points, it is expected that the orbital motion should only exist in the area with the triangle formed by the points at $V = \frac{1}{6}$. When going out of that area the trajectory runs away and shoot off to infinity. To verify this, we found the potential projection and equipotential curves as a visual. This will be further elaborated on in the methodology and results.

What is left to do now before we start our numerical study is to set up our dimensionless Hamiltonian and find the equations of motion. The kinetic energy in (x, y) space has this form,

$$T = \frac{1}{2m}p_x^2 + \frac{1}{2m}p_y^2 \tag{26}$$

We apply the following transformation using the dimensions when we transformed the potential energy.

$$\begin{aligned} p_x &= mL\omega p_x' \\ p_y &= mL\omega p_y' \\ T &= mL^2\omega^2 T' \end{aligned} \tag{27}$$

The kinetic energy becomes,

$$\begin{aligned} T &= \frac{1}{2m}p_x^2 + \frac{1}{2m}p_y^2 \\ mL^2\omega^2 T' &= \frac{1}{2}mL^2\omega^2 p_x'^2 + \frac{1}{2}mL^2\omega^2 p_y'^2 \\ T' &= \frac{1}{2}p_x'^2 + \frac{1}{2}p_y'^2 \end{aligned}$$

$$T = \frac{1}{2}p_x^2 + \frac{1}{2}p_y^2 \tag{28}$$

So, to obtain our Hamiltonian, we add equations 28 and 11

$$H = \frac{1}{2}p_x^2 + \frac{1}{2}p_y^2 + \frac{1}{2}x^2 + \frac{1}{2}y^2 + x^2 y - \frac{y^3}{3} \tag{29}$$

Using Hamilton's equations, we can find the equations of motion of the system.

$$\begin{aligned} \dot{x} &= \frac{\partial H}{\partial p_x} = p_x \\ \dot{p_x} &= -\frac{\partial H}{\partial x} = -x - 2xy \end{aligned} \tag{30}$$

$$\begin{aligned} \dot{y} &= \frac{\partial H}{\partial p_y} = p_y \\ \dot{p_y} &= -\frac{\partial H}{\partial y} = -y - x^2 + y^2 \end{aligned} \tag{31}$$

Therefore, the coupled equations of motion governing our system is,

$$\begin{aligned} \ddot{x} &= -x - 2xy \\ \ddot{y} &= -y - x^2 + y^2 \end{aligned} \tag{32}$$

With all of these our stage is now set to commence and work on our numerical simulations and analysis.

3 Methodology

We approached this system carefully and attacked it numerically. First, we worked with the potential and visualize it by plotting it and projecting it on the xy plane. This helped us see where the potential is bounded and where is diverges along with the fixed points.

```
x = syp.Symbol("x")
y = syp.Symbol("y")
def V(x, y):
    return (1/2)*(x**2 + y**2) +
            (x**2 * y - (y**3/3))
plot3d(V(x,y), (x, -0.3, 0.3), (y, -0.3, 0.3))
syp.plot(V(0, y), (y, -0.3, 0.3))
syp.plot(V(x, 0), (x, -0.3, 0.3))

def potential(x,y):
    return (1/2)*x**2 + (1/2)*y**2
            + x**2 * y - (y**3)/3

x = np.linspace(-1.5, 1.5, 500)
y = np.linspace(-1.5, 1.5, 500)
X, Y = np.meshgrid(x, y)
U = potential(X, Y)

plt.figure(figsize = (10, 7.5))
plt.contourf(X, Y, U, levels = 100,
    alpha = 0.8, cmap = 'gist_earth')
color_bar = plt.colorbar()
color_bar.set_label('Potential')

contours = plt.contour(X, Y, U, colors = 'k',
```

```
levels = 100, alpha = 0.8, linewidths = 0.5)
    plt.clabel(contours, inline = True,
    fontsize = 8)

    triangle = plt.contour(X, Y, U,
    colors='r', levels=[1/6], linewidths=2)
    plt.clabel(triangle, inline = True,
        fontsize = 8, colors = 'k')
    plt.scatter((0, np.sqrt(3)/2,
            -np.sqrt(3)/2), (1, -1/2, -1/2),
        c = 'k', label =
        "Fixed Saddle Points", zorder=10)

    plt.title("Potential Map and
            Equipotential Curves")
    plt.xlabel("x")
    plt.ylabel("y")
    plt.legend()
    plt.show()
```

Then, we decomposed the equations of motions into first order differential equations,

$$\begin{aligned}\dot{x} &= v\\ \dot{v} &= -x - 2xy\\ \dot{y} &= u\\ \dot{u} &= -x - 2xy\end{aligned}$$

and we solved it using Runge-Kutta 4 starting with initial conditions $x = 0$ and $\dot{y} = 0.3$, and we varied the initial y by taking random values between -0.3 and 0.3. We found the initial velocity in the x-direction by using the first integral of motion. We did it for three different energies $E = (1/12, 1/8, 1/6)$.

```
    def system(t, z):
        x = z[0]
        v = z[1]
        y = z[2]
        u = z[3]
        dxdt = v
        dvdt = - 2 * x * y - x
        dydt = u
        dudt = - y - x ** 2 + y ** 2
        dzdt = [dxdt, dvdt, dydt, dudt]
        return dzdt

    yi = np.linspace(-0.3, 0.3, 10)
    print(yi)
    for j in tqdm(range(len(yi))):
        E = 1/8
        x0 = 0
        y0 = yi[j]
        u0 = 0.3
        v0 = np.sqrt(np.abs(2 * E - u0**2 -
        x0**2 - y0**2 - 2 * x0**2 * y0
        + (2/3) * y0**3))
        initial = [x0, v0, y0, u0]
        z = sp.integrate.solve_ivp(system,
        [0, 100000], initial,
        method='RK45', max_step = 0.01)
        t, x, v, y, u = z.t, z.y[0], z.y[1],
        z.y[2], z.y[3]
    # continuation of this code is after
    # we explain Poincare Mapping
```

After obtaining the values of positions and velocities, we constructed the Poincaré map. Trying to apply the conditions of the map proposed in equation (7), we considered the points positive x value that proceed a point that has a negative x value given that the velocity in the x direction is positive,$\dot{x} > 0$, i.e. the points going out of the $x = 0$ plane. Then, we took the midpoint between the two x values assuming that the trajectory while going from negative to positive passes through zero. This only give us values of x near zero, however getting the perfect zero is impossible and this is the most logical way to approach the section. Then, after locating when $x = 0$, we select the values of y and $\dot{y}$ and scattered them for different values of y_0.

```
        ys = []
        us = []
        for i in tqdm(range(len(x)-1)):
            if v[i] > 0 and x[i] < 0 and x[i+1] > 0:
                y_mid = (y[i] + y[i+1])/2
                u_mid = (u[i] + u[i+1])/2
                ys.append(y_mid)
                us.append(u_mid)
        plt.scatter(ys, us, marker= '.', s = 5)
    plt.title(f"E = {E}")
    plt.xlabel("y")
    plt.ylabel("$\dot{y}$")
    plt.show()
```

Lastly, we tried to visualize the trajectories of for different initial conditions, different parts of the Poincaré map, to see how choatic or ordered the trajectories look.

```
    z = sp.integrate.solve_ivp(system, [0, 1000],
    initial, method='RK45', max_step = 0.1)
    t, x, v, y, u = z.t, z.y[0], z.y[1],
    z.y[2], z.y[3]
    fig = plt.figure(figsize = (10, 10))
        if k == 8 or k == 9 or k == 10:
            plt.xlim(-0.6,0.6)
    plt.plot(x, y)
    plt.xlabel('x')
    plt.ylabel('y')
    plt.title(f"Point {k+1}, E = {E}, x0 = {x0},
            y0 = {y0}, px0 = {v0}, py0 = {u0}")
    plt.show()
```

4 Results and Analysis

We start by looking at the potential. We recall that we analytically found the fixed points and their stability, equations (12) through (23), and we theorized that the behavior of the trajectories is bounded. Any trajectory with energy less that $\frac{1}{6}$ is closed and bounded while any that is larger is unbounded and diverges. This is confirmed with the numerical calculation and plotting of the potential. The below figure 4 shows us that the fixed points form a triangle at

$V = 0.1667$. The trajectories of the energies within this triangles are closed and get more circular as you approach the center, whereas the equipotential curves for energies larger than $V = 0.1667$ open and exit channels appear where the particle may escape to infinity.

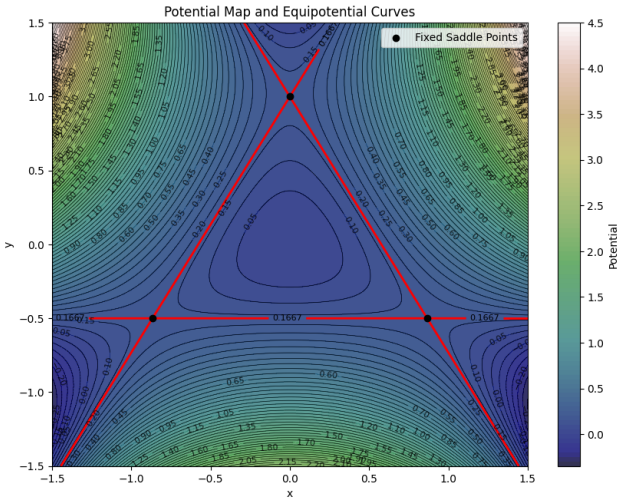

Figure 4: Potential Map and Equipotential Curves

Figure 5 shows the phase space sectioned at $x = 0$ and $\dot{x} > 0$ for the given value $E = \frac{1}{12}$. Points with the same colors correspond to one computed trajectory for one of the initial conditions. In every case, for different initial conditions, all the points lie exactly on a curve, and these curves fills all the available area of the space. A closed curve indicates a periodic trajectory. Since all the points lie on one of the curves, this indicates that an isolating integral of motion exists.

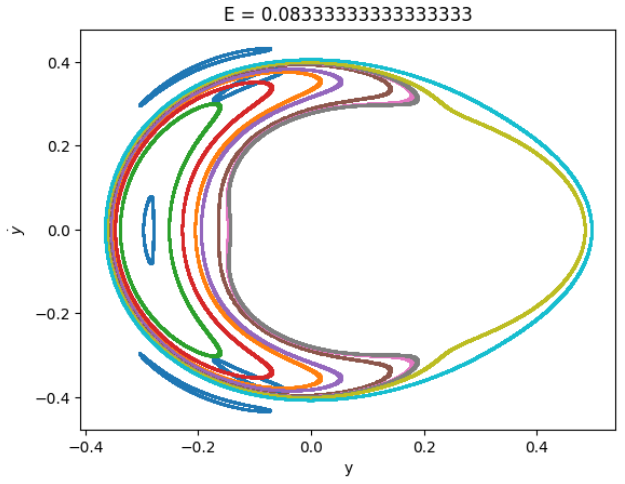

Figure 5: Poincaré Map when $E = \frac{1}{12}$

Figure 6 below corresponds to a higher energy, $E = \frac{1}{8}$. We can observe that we still see the closed curves around stable points; however, they don't fill the whole area. We can see that more points are isolated and they don't follow a certain curve and it fills the whole available area. They behave in a different way. The little five loops on the right of the picture belong to the same trajectories. The points jump from one loop to the next successively. Those loops are called islands, and the collection of the islands, like the five on the right or the four on the top and bottom of the diagram, is called a chain of islands. Each chain corresponds to a periodic motion around a stable point. We can also observe and conclude that the dimensions of the islands decreases rapidly when the number of islands increase. The mixture of closed curves and ergodic trajectory allude that the isolating integral of motion that we are looking for might be absence for certain initial conditions and exists for others.

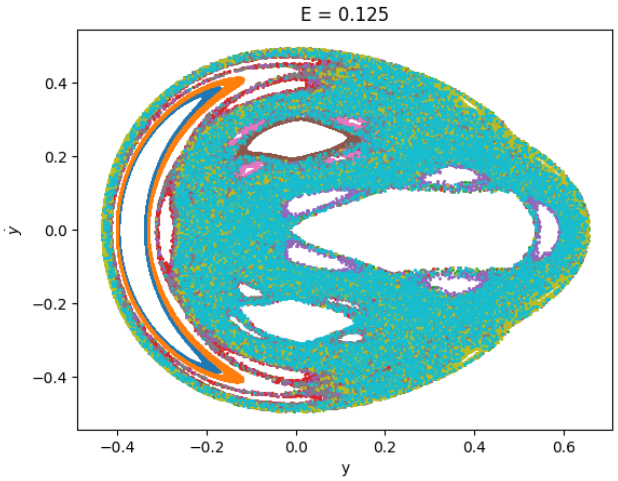

Figure 6: Poincaré Map when $E = \frac{1}{8}$

Figure 7 shows the phase space $(y, \dot{y})$ for energy $E = \frac{1}{6}$. The picture changes dramatically. Almost all initial conditions led to ergodic trajectory and filled up the whole available area. Most of the closed curves from figure 6 disappeared. It can be assumed that their central invariant point became unstable. The other two set of closed curves, on the left and right of the picture in figure 6, have transformed each into a chain of two small islands. A new trajectory is shown in figure 7, an intermediate trajectory between closed curves and ergodic. The points are situated in the middle of the area forming the eight shape that we see. One of the hypothesis Hénon and Heiles proposed while analysing this behavior is that after some time following a closed curve, the points will start penetrating into the ergodic region. This further proves that the isolated integral existence depends on the initial conditions.

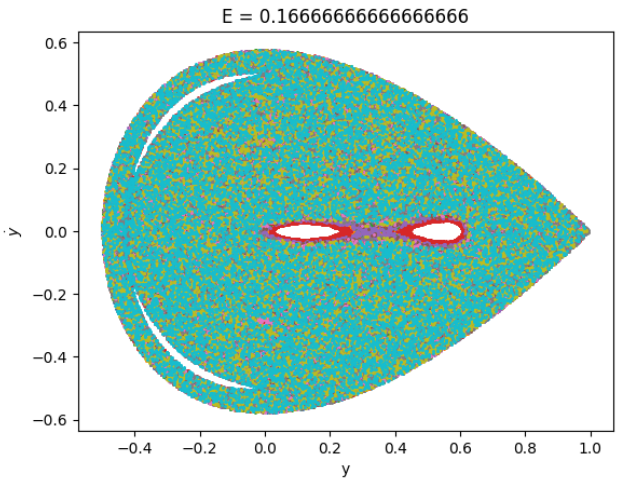

Figure 7: Poincaré Map when $E = \frac{1}{6}$

A remarkable feature to point out is the quick and complete change in the phase space portrait over a moderate interval of the energy. For $E = \frac{1}{12}$, the area is completely filled with closed curves, and then when we double the energy where we set $E = \frac{1}{6}$, the closed curves are almost replaced by an ergodic region. This is consistent with the equipotential curves. If the escape potential is $V_{esc} = \frac{1}{6}$ and the orbit is ergodic, a star or an object moving in a potential greater than $\frac{1}{6}$ can escape to infinity, and the area in the $(y, \dot{y})$ plane becomes infinite.

To study the trajectory of the system, we sampled twelve different points from the Poincaré map for $E = \frac{1}{8}$. If a resonant orbit completed m oscillations perpendicular to the x-axis and in the time that it takes the orbit to perform n circuits along the y-axis, it is said that the orbit is a m:n resonant orbit.

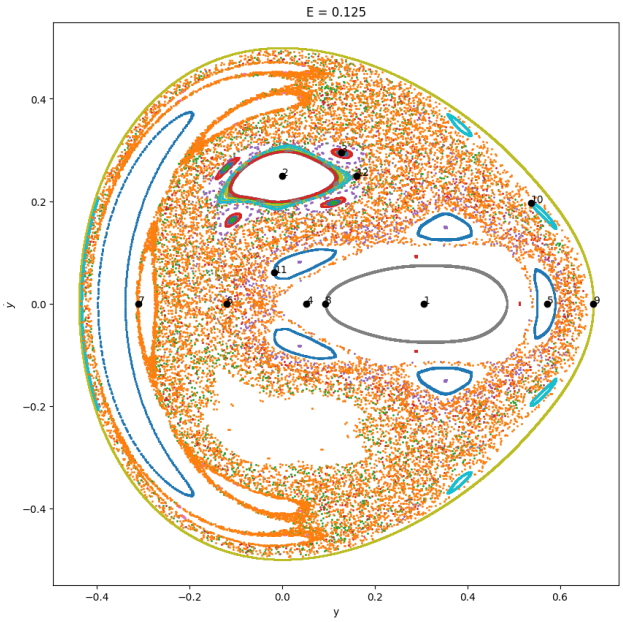

Figure 8: Poincaré Map for $E = \frac{1}{8}$ with Numbered Points

Points 1 and 2 were sampled from the middle of the big closed loops in area. Their trajectories, figures 9 and 10, are periodic with 1:1 resonance. Point 1 has a loop orbit while point 2 has a linear orbit.

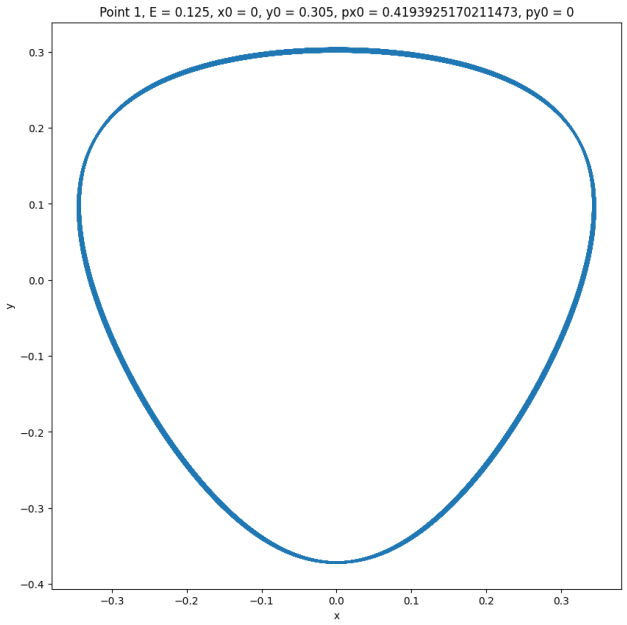

Figure 9: Trajectory of Point 1

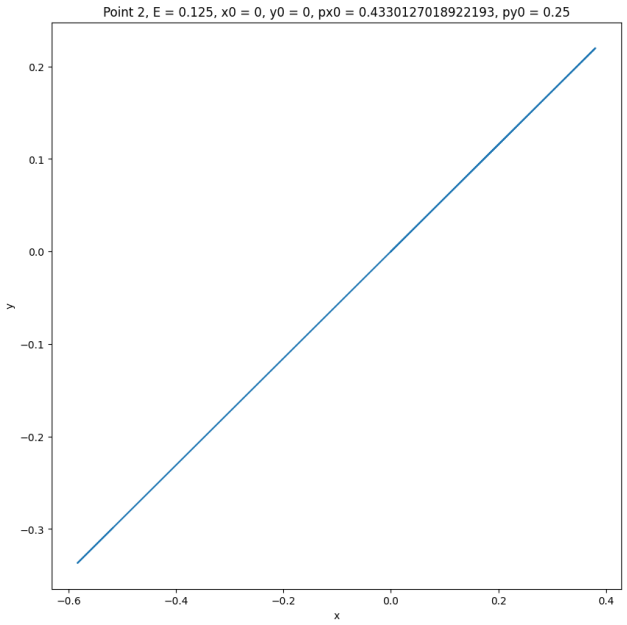

Figure 10: Trajectory of Point 2

While point 3 and point 4 were sampled from one of the four islands and one of the small crescents in the vicinity of the oval exclusion zone around point 1 respectively. Both of their trajectories, figures 11 and 12, show a periodic 5:5 resonant orbit.

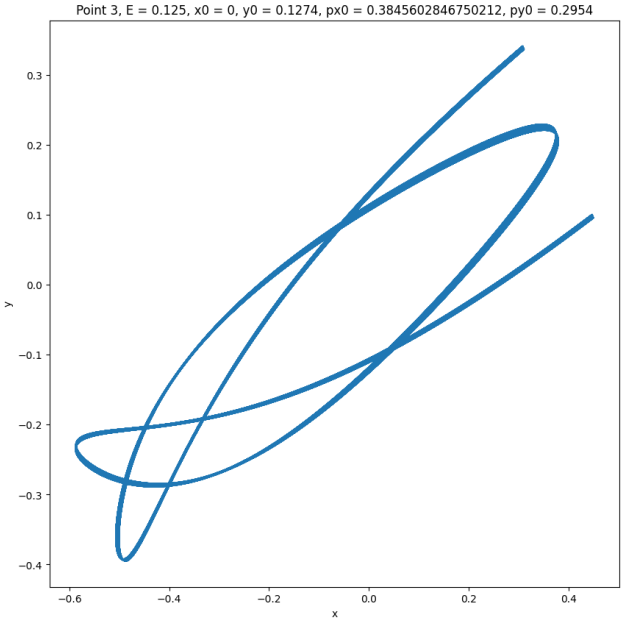

Figure 11: Trajectory of Point 3

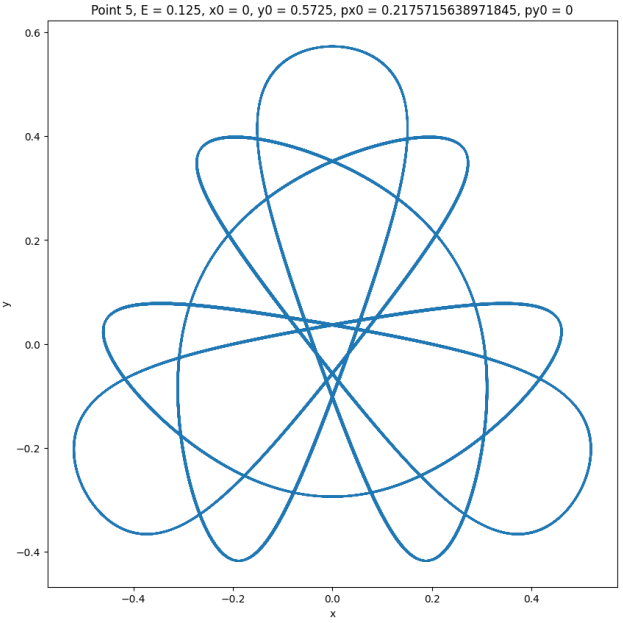

Figure 13: Trajectory of Point 5

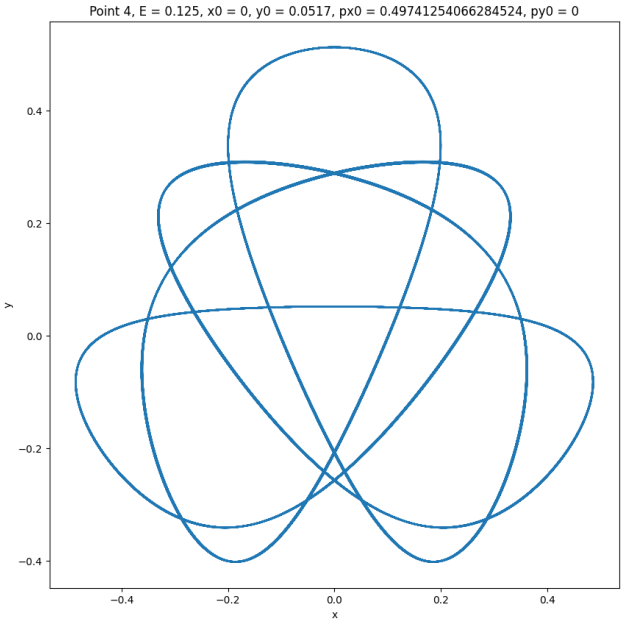

Figure 12: Trajectory of Point 4

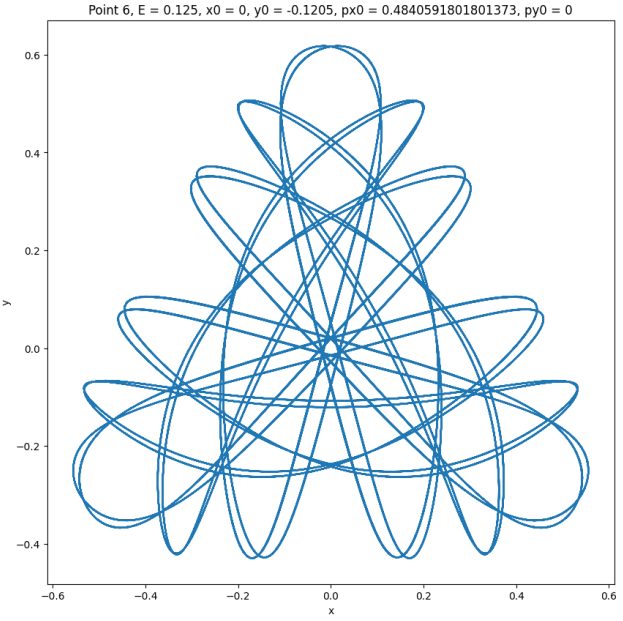

Figure 14: Trajectory of Point 6

Point 5 is sampled from one of the five islands in the middle chain. Its trajectory, figure 13, shows a periodic 5:5 resonant orbit. As we can see from points 3 and 5, the ratio between the number of oscillations depends on the number of islands in the chain. The chain of point 3 has four islands and its periodic ratio is 4:4, while the chain of point 5 has five islands and its periodic ratio is 5:5. This is another characteristic of the islands. Point 6 is sampled from one of the ergodic areas of the map. We can see that its trajectory, figure 14, is starting to lean to chaotic behavior and stray away from the perfect periodic behavior.

Points 7, 8, and 9 are sampled from the boundary of the closed loops. The trajectories of points 7 and 8, figures 15 and 16, are periodic with complex resonance ratio. They have 5:25 and 11:37 periodic orbits respectively. Whereas, the trajectory of point 9, figure 17, may seem period, but it isn't fully periodic. It is quasi-periodic with quasi-period equal to 4.

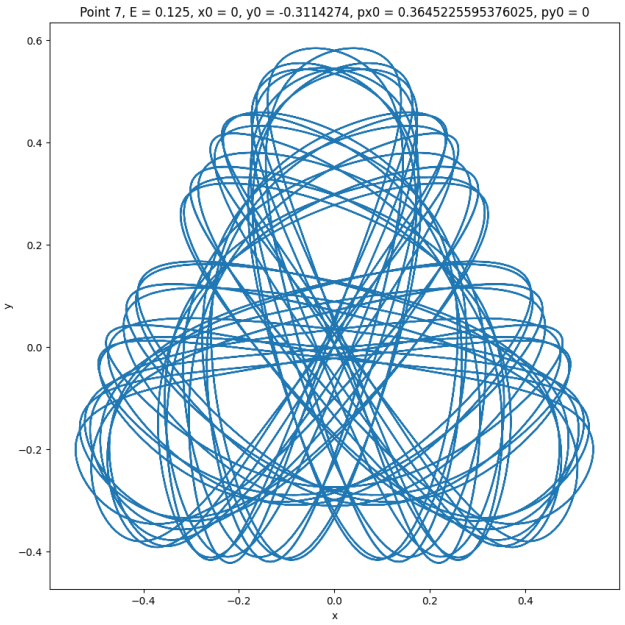

Figure 15: Trajectory of Point 7

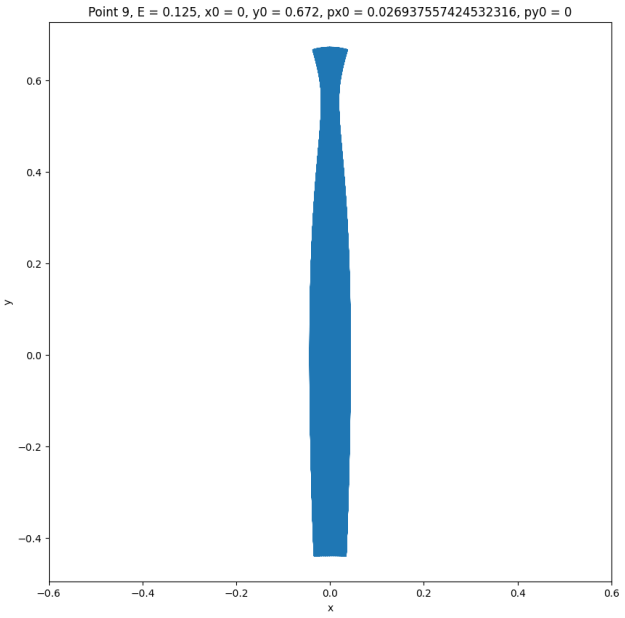

Figure 17: Trajectory of Point 9

Points 10 and 11 were sampled from the boundaries of the islands in the chains. Both trajectories, figures 18 and 19, have a quasi-periodic orbit. The trajectory of point 10 has a quasi-period of 5 while the trajectory of point 9 has a quasi-period of 5 in x and that of 5 and high order repeats in y. Lastly, point 12 was sampled from one of the highly dense ergodic area, and as expected its trajectory, figure 20, is fully chaotic with no hint of periodicity.

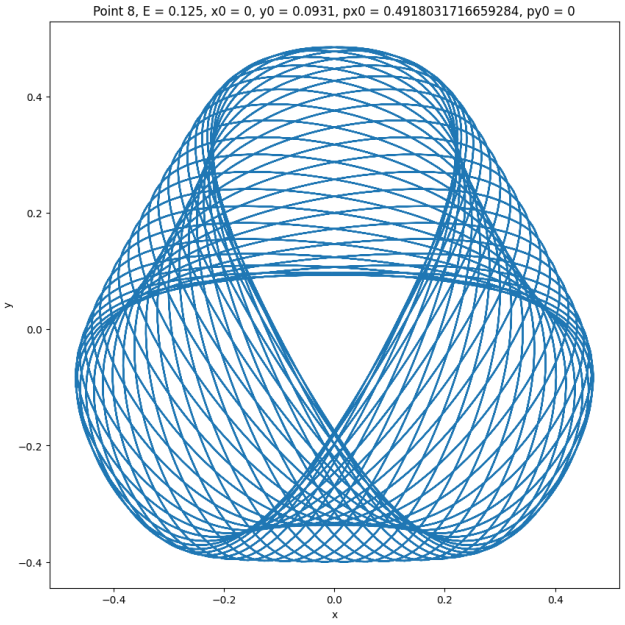

Figure 16: Trajectory of Point 8

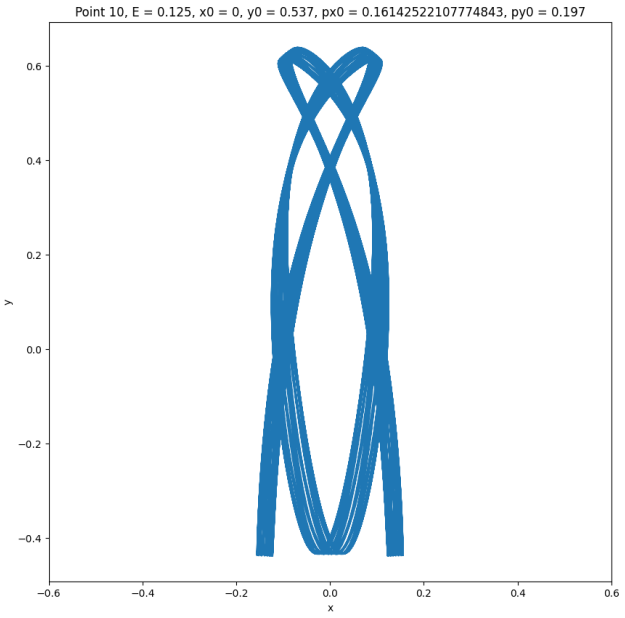

Figure 18: Trajectory of Point 10

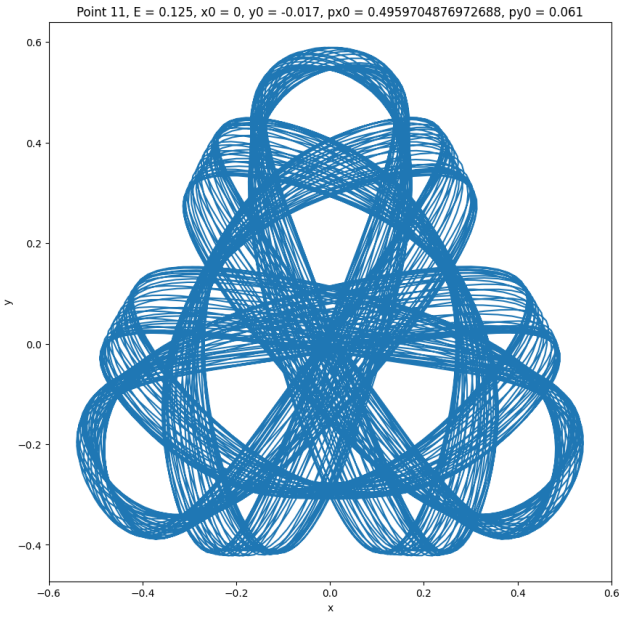

Figure 19: Trajectory of Point 11

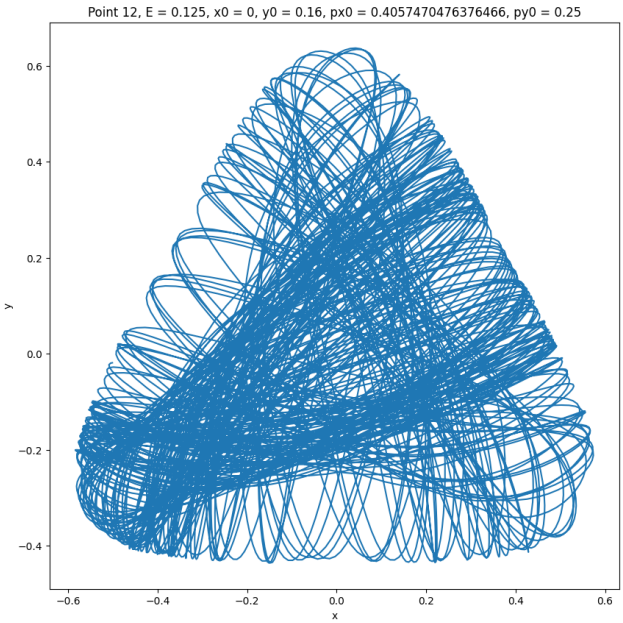

Figure 20: Trajectory of Point 12

5 Conclusion

All in all, the numerical experiments showed that the behavior of this system is complicated and complex, so trying to find an explicit answer whether a third isolating integral of motion exists or not. However, for a given potential and momenta, the integral of motion seemed to exist for a set of initial conditions under a critical energy. In the Hénon Heiles potential, if the energy was under the escape value $V_{esc} = \frac{1}{6}$, then the possibility of the integral existing is higher depending on the initial conditions of the system. For very low energies, the possibility of having a third isolating integral is higher than high energies. Additionally, the trajectories and orbit produced by the system is very diverse and complex. There are a large variety of resonant orbits. On the other hand, there are also extended chaotic domains that separates the area of regularity and periodicity. This system is complex, chaotic, and diverse.

References

Henon, M., & Heiles, C. (1964). The applicability of the third integral of motion: Some numerical experiments. *The Astronomical Journal, 69(1)*, 73–79. https://doi.org/10.1086/109234

Regev, O. (2012). Stellar orbits in a model galactic potential. *In Chaos and complexity in Astrophysics* (pp. 21–28). chapter, Cambridge University Press.

Zotos, E. E. (2014). Classifying orbits in the classical Hénon–Heiles hamiltonian system. *Nonlinear Dynamics, 79(3)*, 1665–1677. https://doi.org/10.1007/s11071-014-1766-6